A system-wide analysis of lipid transfer proteins delineates lipid mobility in human cells

Kevin Titeca[1,2,#], Antonella Chiapparino[2,#], Dénes Türei[3], Joanna Zukowska[2], Larissa van Ek[1], Mahmoud Moqadam[4,5], Sergio Triana[2], Inger Ødum Nielsen[6], Charlotte Gehin[2,^^], Kenji Maeda[6], Theodore Alexandrov[2], Julio Saez-Rodriguez[3], Nathalie Reuter[4,5], Marco L. Hennrich[2,^,*], Anne-Claude Gavin[1,*]

[1]*Department of Cell Physiology and Metabolism, University of Geneva, Geneva, Switzerland.*

[2]*European Molecular Biology Laboratory, EMBL, Heidelberg, Germany.*

[3]*Faculty of Medicine, and Heidelberg University Hospital, Institute for Computational Biomedicine, BioQuant, Heidelberg University, Heidelberg, Germany*.

[4]*Departement of Chemistry, University of Bergen, Norway.*

[5]*Computational Biology Unit, Department of Informatics, University of Bergen, Bergen, Norway.*

[6]*Cell Death and Metabolism Unit, Center for Autophagy, Recycling and Disease, Danish Cancer Society Research Center, Copenhagen, Denmark*.

[^]*Current affiliation, Cellzome GmbH, a GlaxoSmithKline Company, Heidelberg, Germany.*

[^^]*Current affiliation: École Polytechnique Fédérale de Lausanne (EPFL), AI 1108 - Station 19, Switzerland*.

#Equal contribution

**Correspondence and requests for materials E-mail: anne-claude.gavin@unige.ch and marco.x.hennrich@gsk.com.*

Lipid transfer proteins (LTPs) maintain the specialized lipid compositions of biological membranes, and many are associated with disease. In eukaryotes, they support organellar functions by transporting lipids between compartmentalized metabolic pathways. However, for the majority of the hundreds human LTPs, the cargoes remain unknown. We combined biochemical, lipidomic and computational methods to characterize LTP-lipid complexes assembled *in cellulo* and in an *in vitro* biochemical assay. We identified bound lipids for about half of the LTPs analysed, and confirmed known cargoes, while discovering new ones for most LTP families. This work represents a systematic resource that captures the general principles of non-vesicular lipid transport in humans. The specificity of LTP for lipids involves not only the recognition of specific head groups, but also of specific fatty acids. This selectivity defines lipid species within a lipid class with different metabolic or functional fates. The generalized ability of LTPs to form complexes with more than one classe of lipids delineates new relationships between lipids and regulatory mechanisms that may contribute to the coordination of metabolism between different organelles. This work represents a proof of principle and a resource for follow-up analyses in different cell types or following different cellular perturbations or stimulations.

Human cells generate thousands of different lipids[1], the so-called lipidome, whose composition is adapted to cellular needs and functions. It directly influences biological processes, signalling efficiency and contributes to the establishment of cell identity and its functional specialization[2,3]. Importantly, all aspects of lipid function rely on their heterogeneous distribution in biological systems, where lipids accumulate locally and define the membranes of specific organelles or microdomains[4]. Maintaining optimal functional membrane composition involves compartmentalized lipid metabolism, associated with a variety of lipid sorting and transport systems, which can be provided by lipid-transfer proteins (LTPs) [5-9]. LTPs are structurally diverse, but many share a common mode of action: they bind and mobilise lipids into a hydrophobic pocket, forming stable, water-soluble protein-lipid complexes that isolate lipid cargoes from the aqueous phase and enable lipid transport within or between cells (reviewed in [10-12]). In addition to their role in replenishing organelle lipid stores, some also act as chaperones presenting cargo to downstream protein effectors, such as enzymes, or as lipid sensors controlling cell signalling[8,10,13-15].

LTP functions are essential and conserved in all kingdoms of life (reviewed in [16]). There are at least 131 LTPs in humans, whose dysfunction is often associated with various diseases[12,17,18]. However, we only understand the function of a small number of them and for the majority the identity of their cargoes remains elusive. As they have never been systematically studied, we still lack a complete mapping of LTP-mediated lipid transport pathways; how they overlap, cooperate and act synergistically. In previous proof-of-principle studies in a model eukaryote, *Saccharomyces cerevisiae*, we demonstrated the feasibility of systematic analyses of lipid transfer[6]. We therefore set out to characterize human LTP-lipid complexes assembled under physiological conditions in a human cell line and in an *in vitro* biochemical assay. Due to its unprecedented scale, the resulting resource significantly expands our understanding of non-vesicular lipid transport in humans.

A systematic resource for the study of human non-vesicular lipid transport

The lipid binding properties of LTPs have not yet been systematically studied and the general principles of their specificity and functions have remained elusive. Here, we measured the ability of human LTPs to mobilize specific lipid cargoes, i.e. to load them and carry them in aqueous environments. To this end, we have adapted affinity purification methods coupled with lipidomics to characterize soluble LTP-lipid complexes[6], and applied them to two complementary approaches (Supplementary methods). We measured the ability of affinity-tagged LTPs overexpressed in HEK293 cells to associate stably with lipids in the physiological context of a human cell (Fig. 1a; *in cellulo*). We also studied the ability of recombinant LTPs, expressed in *Escherichia coli*, to extract lipids from artificial membranes composed of lipids extracted from bovine liver and porcine brain (Fig. 1a; *in vitro*).

In total, 101 human LTPs were cloned, and we were able to express 86 in HEK293 cells and 71 in *E. coli* (Fig. 1a). We successfully purified 110 LTP-lipid complexes assembled *in cellulo* or *in vitro* (counting the redundancy of two screens) by affinity and size exclusion chromatography (SEC) (Fig. 1a). The SEC fractions were analysed by sodium dodecyl sulfate-polyacrylamide gel electrophoresis (SDS-PAGE) and liquid chromatography-tandem mass spectrometry (LC-MS/MS)- or high-performance thin-layer chromatography (HPTLC)-based lipidomics (Supplementary methods;

Supplementary Data S1A, S1B and S1C; Extended Data Table 1)[6]. To filter out non-specific background, we matched the abundance of LTPs in SEC fractions with that of lipids. Only lipids identified in all fractions containing LTPs and showing an elution profile (i.e., changes in abundance in fractions) similar to that of LTPs were considered as potential lipid binders. The work consisted of more than 600 LC-MS/MS runs, and the analysis of the resulting large datasets required the development of semiautomatic pipelines, incorporating quality filtering and manual processing of the spectra (Fig. 1b and Extended Data Fig. 1) (Supplementary methods). To ensure the accuracy and depth of identification of the different lipid species (for example to characterize the composition of their fatty acid chains), we measured the experimental fragmentation and elution patterns of series of lipid standards to define fragmentation rules (Extended Data Tables 2A and 2B), which we combined with spectral information from the databases METLIN, SwissLipids and LIPID MAPS[19-21]. We also considered evaluating the overall quality of the LC-MS/MS-based analyses[22-25]. As expected from a reverse-phase LC system, lipids with long fatty acids (i.e., more hydrophobic) had longer retention times than those with short fatty acids, whereas lipids with unsaturated fatty acids eluted more rapidly than their saturated counterparts (Extended Data Fig. 2a). The fact that we often identified lipid species in the form of different adducts and in different MS ionization modes also increased confidence in their identification (Extended Data Fig. 2b).

We identified lipid cargoes for 45 of the LTPs that we could affinity purify (Fig. 1a; Extended Data Table 1). The datasets cover nine of the ten LTP families, with up to 10 representatives for the lipocalins[10]. While the majority of LTPs analysed were successfully expressed and purified in both expression systems (HEK293 and *E. coli*), only six acquired lipids in both assays (Fig. 1a). This shows that the two approaches are complementary. The *in cellulo* screen is more likely to capture lipid cargoes of LTPs whose assemblies require a cellular machinery. However, it is also limited to one biology, that of exponentially dividing HEK293 cells, where specific pathways and functions are inactive (see examples below). The *in vitro* approach offers a broader scope, as LTPs are exposed to a wide variety of lipids, but we will miss the lipid cargoes of LTPs whose assembly requires a cellular machinery. The integration of both *in cellulo* and *in vitro* methods provide systematic data on LTP-lipid complexes and represents an important resource.

General properties the LTP-associated lipidome

This is a comprehensive analysis of the lipid-binding properties of human LTPs, and such an extensive study helps to define possible general principles for these proteins. We first investigated whether the lipids recognized by the analysed LTPs differ from the total lipidome, i.e., whether the LTP system shows preferences for certain lipid attributes or properties. For this, we measured the total lipidome of HEK293 cells cultured under the same conditions by LC-MS/MS-based lipidomics and compared it with the lipidome mobilized by LTPs (Fig. 2 and Extended Data Table 5).

We observed well-known patterns, for example the enrichment of lipids in fatty acids with an even number of carbons, in particular 32, 34, and 36, both in the total cellular lipidomes and those associated with LTPs (Fig. 2a,b). Interestingly, the presence of odd-numbered species is more common in LTP-lipid complexes assembled *in vitro* (Fig. 2a and Extended Data Fig. 2c). This likely reflects their exposure to a wider range of lipids, including those of the expression host, *E. coli*, where odd numbered lipids are more frequent[26]. In line with this notion, these exclusively assembled *in vitro* complexes often contain lipids that are abundant in bacteria but not in humans (e.g. phosphatidylglycerol) (Fig. 2b and Extended Data Fig. 2c), suggesting that some may have been assembled in *E. coli*[6]. These *in vitro* data suggest that they insert biochemically into the binding pocket, and are therefore informative as to the nature and extent of this pocket's binding.

We also observed some interesting general trends. The LTPs studied in both screens preferentially mobilized glycerophospholipids with shorter fatty acids, whereas we did not observe a similar trend for sphingolipids, which seem to have more complex selectivity patterns (Fig. 2b) (see below). Similarly, LTPs also showed a preference for glycerophospholipids bearing only one to two sites of unsaturation in their fatty acids (i.e., carrying one or two double bounds) (Fig 2c). These lipid species can cause deep membrane defects, a phenomenon that can contribute to the membrane lipid uptake[27]. In contrast, polyunsaturated fatty acids (PUFAs), and fully saturated fatty acids cause only superficial or no defects, respectively, and may be more difficult to extract from membranes[27].

Importantly, the LTP associated lipidome sometimes reveals lipid species that were barely, if at all, detectable in the total lipidome of HEK293 cells, such as ceramide species with very long acyl

chains (Fig. 2b and Extended Data Table 5) (see below). The enrichment for rare and low-abundant lipids, unlikely to come from nonspecific contamination of the total lipidome, provides an additional level of confidence in the dataset. More interestingly, it also suggests that within the major lipid classes, aliphatic chain lengths and saturation define lipid pools that are differentially accessible to the LTP system and that may experience different metabolic fates (see below).

An LTP-lipid interactome map reveals new routes of lipid transfer

The screens confirmed many of the previously known LTP cargoes (Fig. 3a,b), knowledge that can be used to assess the quality and the complementarity of the two screens (Extended Data Table 1). For example, some of the known associations between LTPs and lipids, such as phosphatidylcholine with STARD2 and STARD10, are observed in both screens, while others are screen-specific. This highlights the unique ability of each approach to detect a different set of complexes. Among the known LTP-lipid complexes observed only *in cellulo* are those whose assembly requires a cellular machinery. For example, the retinol-binding proteins, RBP1 and RBP4 formed complexes with vitamin A only in the cellular context. This is likely because their assembly requires active metabolism and transmembrane transport systems, which are absent in the *in vitro* assay[28].

In other cases, LTPs load their known cargoes only in the *in vitro* biochemical assay, i.e., where they escape spatial or temporal cellular controls and possible contextual imbalances in cellular lipid availabilities[29]. Members of two evolutionary distinct LTP families that transport phosphatidylinositol, the precursor of phosphoinositide (PIP) synthesis, illustrate this situation. SEC14L2 belongs to the CRAL-TRIO family, some members of which are known to transport phosphoinositide from the ER for phosphorylation into specific PIPs that accumulate in the membranes of various organelles, thereby contributing to organelle identity and maintenance[30-32]. While PITPNA, PITPNB and PITPNC1, belong to the phosphatidylinositol transfer protein (PITP) family, and participate in the so-called phosphatidylinositol cycle. They transfer phosphatidylinositol from the ER to the plasma membrane to replenish the phosphatidylinositol pool after signalling via phospholipases C-mediated hydrolysis of PI(4,5)P_2[33]. Although phosphatidylinositol is abundant in HEK293 cells, *in cellulo* we did not find it associated with PITPNs, but with SEC14L2 (Fig. 3a,c and

Extended Data Fig. 3). This is likely because SEC14L2-phosphatidylinositol complexes contribute to important functions in dividing cells that must duplicate their organelles (such as the HEK293 cells used here), whereas phospholipases signalling is probably not active in this cellular context, so PITPs-phosphatidylinositol complexes do not assemble. PITPs formed complexes with phosphatidylinositol but only *in vitro* in the biochemical assay. What is interesting is that it does so primarily with PI(38:4), the arachidonic acid-containing species (Fig. 3c), which is known to be predominant in the phosphatidylinositol cycle[34]. This demonstrates that PITPNA, PITPNB and PITPNC1 in the absence of a cellular have preferences arachidonic acid-containing phosphatidylinositol species, and that this ability is likely to contribute to the metabolic routing of specific fatty acids to the phosphatidylinositol cycle[34].

We also identified lipids for nine LTPs with no previously known ligands: SEC14L6, ATCAY, BNIPL, BPIFB2, SEC14L5, TTPAL, LCN15, SCP2D1, and HSDL2 (Fig. 3a and Extended Data Table 1). For example, BPIFB2 forms *in cellulo* complexes with bismonoacylglycerolphosphate (BMP), a rare lysosomal lipid whose biosynthesis pathways are still elusive, suggesting a possible role in these processes[35]. Hydroxysteroid dehydrogenase like 2 (HSDL2) is a peroxisomal multi-domain LTP[36] (it has a peroxisomal targeting signal) that bound to triacylglycerol *in vitro* (Fig. 3a and Extended Data Table 1), supporting the idea that it plays a role in peroxisomal triacylglycerol transport and metabolism. Consistent with this hypothesis, the knockdown of HSDL2 leads to the accumulation of lipid droplets[37,38] and several of the known HSDL2 interactors are peroxisomal and involved in β-oxidation (Extended Data Fig. 5a,b). OSBP9 belongs to the family of oxysterol binding proteins. Members of this family are known to exchange phosphatidylinositol-4-P with sterols or with phosphatidylserine between cell membranes[6,39-41]. OSPB9 binds to phosphatidylserine *in cellulo* (Fig. 3a and Extended Data Table 1), consistent with the prediction of a phosphatidylserine-binding motif in its lid region[6].

We even identified lipids, such as BMP or triacylglycerol (see above), that are novel in the LTP transport system. Another example is diacylglycerol, which formed cellular complexes with SEC14L2, a lipid chaperone acting as lipid-presenting scaffold for several lipid kinases, e.g. the phosphatidylinositol 4- kinase[42], the phosphatidylinositol 3- kinase or an as yet unidentified alpha-tocopherol (vitamin E) kinase[43]. As expected, SECL14L2 formed *in cellulo* complexes with

phosphatidylinositol (see above and Extended Data Fig. 3), with a vitamin E-like lipid covalently bound with a carbon structure that does not correspond to fatty acids or squalene, and, interestingly, rare diacylglycerol species (DAG(32:1) and DEG(34:2)) *in cellulo* (Extended Data Fig. 3). This association with diacylglycerol may provide a molecular mechanism for SEC14L2-dependent coordination of phosphatidylcholine biosynthesis (via CDP-choline, i.e., using diacylglycerol as a precursor) with SEC14-mediated stimulation of phosphatidylinositol 4-kinase activity[44]. In this perspective, it is intriguing that diacylglycerol is also the substrate of a family of ten kinases, diacylglycerol kinases, which produce phosphatidic acid. Overall, these examples illustrate that integrating *in cellulo* and *in vitro* approaches to study LTP-lipid complexes in a systematic manner uncovers many new potential lipid cargoes, which should inspire and trigger future work.

Lipid transfer proteins can bind to more than one class of lipid

A few LTPs, such as members of the OSBP, PITP or the CRAL-TRIO families, are known to accommodate more than one class of lipid and this property contributes to the coordination of metabolism between different organelles. Some directly exchange lipids, for example, cholesterol in the ER for PI4P in the Golgi[8,13,39]. For others, the binding of a sensor or regulatory lipid (i.e. phosphatidylcholine for SEC14L2) in a deep pocket initiates various chaperonin functions and the presentation of other lipid (i.e. phosphatidylinositol) to downstream enzymes (e.g., kinases) [44]. Here, we demonstrate that many (22) of the (39) LTPs studied were capable of forming complexes with more than one class of lipid, suggesting that these regulatory mechanisms represent general attributes of LTP functions (Fig. 4).

We reasoned that lipid pairs mobilized by the same LTPs should share physiological relationships. Therefore, we evaluated the links of these pairs in other lipidomics data, specifically whether they are more frequently co-regulated and co-localised than any other random lipid pairs. For this, we integrated data describing changes in lipid abundance following systematic knockdown of enzymes from sphingolipid metabolism[2] (Fig. 5a), and scored all lipid pairs for their co-regulation. In this scoring system, a “+1.0” denotes perfect co-regulation (lipids always change abundance in the same way), whereas a “-1.0” denotes mutual exclusion (lipids always change oppositely). We also

exploited a large spatial metabolite database, METASPACE, which consists of thousands of tissue sections analysed by imaging mass spectrometry (Fig. 5b). Each pixel in these images corresponds to one mass spectrometry analysis (Supplementary methods)[45]. Finally, we also included a dataset capturing the lipidome of affinity-purified organelles, to refine lipid co-localisation to subcellular levels (unpublished data) (Fig. 5c). For all lipid pairs in these datasets, we determined their co-occurrence by the Manders' overlap coefficient[46] (Supplementary Methods)(Fig. 5b,c). In this system, "+1.0" and "0.0" represent lipid pairs that always or never co-localize, respectively. Interestingly, we observed that the lipid pairs mobilized by the same LTPs are significantly more co-regulated upon metabolic perturbation (Fig. 5a) and co-localised (Fig. 5b,c) than would be expected from random sets of lipid pairs (Extended Data Table 4). These trends remain significant, when only lipid classes are considered, i.e. when excluding closely related lipid species or lipid sub-classes from this analysis (Fig. 5 and Extended Data Fig. 4). Overall, this supports the idea that LTPs can be organized into functional cellular networks linking distinct organelles and contributing to the coordination of metabolism between different cellular compartments.

Interaction map reveals new principles of sphingolipid transport

We identified the expected cargoes for LTPs known to mediate the intracellular movement of several sphingolipids[5,47,48] (Extended Data Table 1). CERT bound ceramides (Fig. 3a), consistent with its contribution to their transport from the ER[5,49,50], where they are made, to the Golgi, where they are metabolized to sphingomyelin, ceramide-1-phosphate or glycosphingolipids[51-53]. GLTPD1 forms complexes with ceramide 1-phosphate[54], and GLTP with glycosphingolipids[53,55-57] (hexosylceramides) (Figs. 3a), which is known to trigger their transport to the plasma membrane. In addition to these well-known examples, we have seen that a lipocalin, LCN1, binds to sphingomyelin (Fig. 3a), a lipid previously not known to be part of this LTP system, as well as to phosphatidylcholine, another choline-containing lipid (Fig. 3a). LCN1 is the major lipid-binding protein in tears, a fluid indeed highly enriched in phosphatidylcholine and sphingomyelin[58].

The acyl chain length of ceramides is exquisitely controlled, and there are six ceramide synthases in mammals that produce ceramides with specific acyl chain distributions[47]. We noted that

CERT exhibits interesting patterns of *in cellulo* specificity for distinct ceramide species, which appears to define different pools with distinct metabolic fates (Fig. 6a). For example, it forms *in cellulo* complexes with rare, saturated and very long – 46 and 48 carbons (long chain base and fatty acid length) – dihydroceramides and phytoceramides (Fig. 6a). Dihydroceramides are metabolic intermediates, produced directly by ceramide synthases, that can be converted to ceramides or phytoceramides by the addition of a double bond or a hydroxyl group at position c-4, respectively[59-61]. This suggests a novel role for CERT in the early sorting of very long-chain dihydroceramides, i.e. prior to conversion to ceramides, for the production of phytoceramides, which are believed to play important structural function in the maintenance and stability of ordered membrane microdomains[62].

Interestingly, *in cellulo*, the 40- to 42-carbon ceramides produced by ceramide synthases 2 and 3[63], although abundant in HEK293 cells, are not mobilised by CERT (Fig. 6a), which is consistent with previous *in vitro* data[50]. These 40- to 42-carbons structures are particularly abundant in the pool of glycosylated ceramides, i.e., those that have acquired hexoses and that are handled by GLTP (Fig. 6a), consistent with the idea that they were transported to the Golgi by a mechanism independent of CERT[5,64]. In contrast, CERT efficiently mobilized the 32- to 36-carbons ceramides. These structures are abundant in the sphingomyelin and ceramide 1-phosphate pools that are handled by GLTPD1 and GLTP, respectively (Fig 6a). To further investigate the role of CERT in ceramide sorting, we measured the impact of its gain of function on cellular lipidomes (Fig. 6b). We observed that over expression of CERT in HEK293 resulted in an increase in cellular sphingomyelin and ceramide 1-phosphate, and a decrease in hexosylceramides. Overall, these data support the idea that CERT is part of a ceramide triage system, thus defining three pools of ceramides with different metabolic fates.

We also observed novel lipid binders for the known sphingolipid transporters, suggesting the existence of novel regulatory mechanisms. For example, GLTPD1, consistently formed complexes not only with its cognate cargo, ceramide 1-phosphate[54], but also with sphingomyelins both *in cellulo* and *in vitro* (Figs. 3a and 6a). Sphingomyelins did not appear to be actively transported by GLTPD1 in *in vitro* transfer assays[54] (data not shown). The function of these complexes with sphingomyelins remains elusive. They may play regulatory roles, for example, by coordinating ceramide 1-phosphate

metabolism (phosphorylation/dephosphorylation) to local sphingomyelin requirement and availability. The other example is CERT, which, in addition to ceramide species also associates with phosphatidylcholine (Fig. 3a). Binding of phosphatidylcholine (palmitoyl-oleoyl-phosphatidylcholine, POPC) to CERT through insertion of one fatty acid tail into its lipid binding pocket was also observed in molecular dynamics simulations of the CERT-START domain with membranes using an all-atoms model[65]. Simulations of the CERT-phosphatidylcholine adducts in the presence and absence of the cargo ceramide in an aqueous environment resulted in both cases in the formation of stable complexes where the hydrophobic cavity accommodates the two lipid tails from the phosphatidylcholine, also in the presence of ceramide (Fig. 6c,d). Phosphatidylcholine is one of the two substrates (with ceramide) of the sphingomyelin synthase that transfers the phosphocholine head of phosphatidylcholine to ceramide. This is consistent with the idea that CERT could act as a chaperone, a notion already proposed for the CRAL-TRIO family[42], bringing both substrates at the same location, and coupling or coordinating their transfer to their transformation in sphingomyelin.

Discussion

By combining two complementary approaches, this study systematically highlights lipid specificities for the numerous human LTPs. This combination elucidates both lipid binding as a function of cellular context and identifies lipids that accommodate into lipid-binding pockets. This is an extensive resource that should enhance our understanding of the pathways linking different parts of lipid metabolism to signalling. The breadth of this research has identified general and specific features for the lipids observed with LTPs, including previously unknown unifying patterns. Comparison of the whole-cell lipidome with that associated with LTPs revealed that not all lipid species are easily manipulated by LTP systems. These showed a general preference for short, single or double unsaturated lipids, known to create deep defects in membrane[27], which should contribute to their extraction from membranes. Different lipid species within the same class will therefore have different mobility in cellular systems. The work has provided novel concepts and important resources, as well as new bioinformatics pipelines for matching protein and lipid elution profiles, and for identifying protein-bound lipids, with the establishment and use of highly detailed spectral rule sets. They are relevant to the wider field of lipid-protein interaction research, and provide a starting

point for extending such analyses to different cell types or following different cell perturbations or stimulations.

The study confirmed many previously known lipid binding partners, but also identified new ones, opening up new avenues of research. The role of lipid headgroups in the specificity and mechanism of lipid transfer has long been recognized. We have observed, for example, that LCN1 binds lipids with a choline head group, while the type of fatty acid linkage (ether or ester), their length or the even the class of lipid (sphingomyelin or phosphatidylcholine) appear to play little role in the recognition mechanisms. Due to the unbiased nature of our assays, where LTPs select lipids from whole lipidomes comprising all species (which has rarely been done to date), we can start assessing specificity beyond lipid head groups. These data suggest that within a lipid class, LTPs have preferences for specific species, and that this selectivity defines lipids pools with different metabolic fate and/or cellular functions.

Most LTPs associate with multiple lipid classes, while this was previously only known for a few of them, this work now supports the notion that this is a general attribute shared by many LTPs. Integration with different types of lipidomics datasets further validated the functional relevance of co-transported lipid pairs. Interestingly, this is significant not only for related lipid species (i.e. lipids with structural similarity or belonging to the same metabolic pathways), but also for lipid classes with no structural and metabolic relatedness. This confirms the idea that lipid co-transport represents an important, but hitherto underestimated, mechanism for the organization and integration of lipid metabolic pathways and the maintenance of organellar membrane function.

Figure legends:

Figure 1: Synopsis of the screens. A: Overview of the analysis steps of the *in cellulo* and *in vitro* screens and the associated success rates. B: Data analysis pipeline overview.

Figure 2: Characterization of the mobilized lipidome of the screens, with a focus on different lipid parts. Focus on the lipids observed with mass spectrometry. (a) Total fraction of the intensities with an even versus odd total carbon chain length of the fatty acyls for the *in cellulo* and *in vitro* screens,

and distribution of the total sum of the intensities for all total carbon chain lengths of the fatty acyls in the *in cellulo* and *in vitro* screens. (b) Normalized intensities distribution of all observed combinations of headgroups and total carbon chain lengths of the fatty acyls. Comparison of the *in cellulo* (blue) and *in vitro* (orange) distributions of the mobilized lipids with the lipids present in the whole HEK293 cells (grey) (Extended Data Table 5) (vitamins were not included). (c) Distribution of total summed intensities for each of the different unsaturation degrees of the fatty acyls for the *in cellulo* and *in vitro* screens.

Figure 3: Overview of the lipids mobilized by the LTPs. (a): Normalized intensities for all observed LTP-lipid subclass combinations for the *in cellulo* and *in vitro* screens, and an overview of their individual novelties. HPTLC-based observations are only represented when no mass spectrometry data was available (black bordered blue triangles). The LTPs were seriated by the presence and location of all of their protein domains, and grouped along the LTP family lines (Extended Data Fig. 4). (b) General number of known and novel LTP – lipid subclass pairs for the *in cellulo* and *in vitro* screens. (c) Distribution of lipid species for PI, PC and PA for the PITP-family of LTPs. The observed intensities of the individual species are normalized to the maximum observed for the specific LTP – lipid subclass pair. The *in cellulo* (filled blue) and *in vitro* (filled orange) distributions for the LTPs are compared with distribution of the lipids present in the whole HEK293 cells (Extended Data Table 5) (grey border).

Figure 4: Most LTPs mobilize multiple lipid subclasses, and most lipid sub-classes are also mobilized by multiple LTPs. (a) Overview of all LTP – lipid sub-class pairs for the *in cellulo* and *in vitro* screens. HPTLC-based observations are only represented when no mass spectrometry data was available (black squares on top of blue squares). The LTPs were seriated by the presence and location of all of their protein domains, and grouped along the LTP family lines (Extended Data Fig. 4). (b) General distribution of the number of LTPs binding different amounts of subclasses for the *in cellulo* and *in vitro* screens.

Figure 5: Co-mobilized lipids by LTPs are also co-regulated and co-localized. Vertical lines in the graphs represent medians. Significant shifts of the observed medians are indicated by a star (see

Extended Data Table 4 for significance calculations). The expected distribution lines in grey are always based on all entries in the reference database, while the expected distribution lines in colour are only based on the observed lipid classes from the reference database by either the *in cellulo* (blue) or *in vitro* (orange) screens. The densities with Gaussian kernels use bandwidth selection according to[66]. An overall density of 1 would correspond to a uniform distribution. All densities have the same surface area for all comparisons within each panel. (a) Comparison of the co-mobilization of lipids by the LTPs with the co-regulation of these lipids, according to the correlation of the lipid abundance changes upon cellular perturbations as described in[2]. (b) Comparison of the co-mobilization of lipids by the LTPs with the Manders' co-occurrence of these lipids in tissue section in the METASPACE database[45,46]. (c) Comparison of the co-mobilization of lipids by the LTPs with the Manders' co-occurrence of these lipids in sub-cellular fractions[46].

Figure 6: Comparison of the species distributions of the sphingolipid mobilizing LTPs for the *in cellulo* (full blue) and *in vitro* (full orange) distributions of the mobilized lipids with the lipids present in the whole HEK293 cells (Extended Data Table 5) (grey border). The observed intensities of the individual species are normalized to the maximum observed for the specific LTP – lipid subclass pair. The data of all hexosyl-containing sphingolipids were integrated into xHexCer. The bottom highlights the specificity of each ceramide synthase (CERS) [63]. (a) Overview of the sphingolipid total acyl chain lengths transported by CERT, GLTPD1 and GLTP. At the top: mobilization by CERT of short-to-medium length d ceramides and long saturated non-d ceramides. Ceramide mobilization by CERT is absent for acyl chain lengths downstream of CERS2,3 and potentially 4. In the middle: broad SM mobilization by GLTPD1 in a similar pattern to the mobilized ceramide-1-phosphate (Cer1P. At the bottom: mobilization by GLTP of hexosyl-containing species with a preference for longer total carbon chain lengths. (b) The effect of overexpression of CERT in HEK293 cells on the cellular lipid class abundances. (c and d) Molecular dynamics simulations show that the START domain can accommodate a phosphatidylcholine (POPC) in its hydrophobic cavity, both in the absence (c) or the presence (d) of ceramide (Supplementary Methods). Ceramide coloured yellow, POPC coloured cyan, Ω1 coloured red and Ω4 coloured blue. START domain is shown as cartoon and coloured grey. Abbreviation: POPC, palmitoyl-oleoyl-phosphatidylcholine.

Acknowledgements

We are grateful to the EMBL Metabolomics core facility; the Proteomics platform of the University of Geneva, and the READS platform of the University of Geneva, for expert help. We acknowledge Lipotype for expert lipidomics analysis. The thank Howard Riezman, University of Geneva, and Emmanuel Varesio, University of Geneva, for inspiring discussions and for sharing their lipidomics expertise. We are grateful to Bernd Klaus, EMBL, and Matt Rogon, EMBL, for sharing their expertise in bioinformatics and statistical data analysis and to Vladimir Rybin, EMBL, for expert help with protein purification. We are grateful to Enric Mila Vilalta who ran the *in vitro* lipid binding assay and Michal Varga for the subcloning of LTPs in the mammalian expression vector. We thank Martin Beck for sharing expression vectors. We also thank members and former members of ACG's groups at the Department of Cell Physiology and Metabolism, University of Geneva and European Molecular Biology Laboratory, EMBL for continuous discussions and support, especially, Emeline Galster (University of Geneva). ACG acknowledge the financial support of the Louis-Jeantet foundation. KT was supported by the EU Marie Skłodowska-Curie Actions project 843407, LipTransProMet.

Author contribution

ACG, AC, MLH designed the research; KT, DT, ACG, TA and JSR designed the data integration and analysis strategy; AC, JZ, LvE and C.G. conducted the molecular biology, cell biology and biochemistry experiments; MLH, IØN, KM conducted the mass spectrometry analyses and with KT interpreted their data; KT, DT and ST performed the bioinformatic analysis; MM and NR performed and interpreted the molecular dynamics experiment; KT and ACG wrote and all authors reviewed the manuscript.

References

1 van Meer, G., Voelker, D. R. & Feigenson, G. W. Membrane lipids: where they are and how they behave. *Nat Rev Mol Cell Biol* **9**, 112-124 (2008). https://doi.org:nrm2330 [pii] 10.1038/nrm2330.

2 Koberlin, M. S. *et al.* A Conserved Circular Network of Coregulated Lipids Modulates Innate Immune Responses. *Cell* **162**, 170-183 (2015). https://doi.org:10.1016/j.cell.2015.05.051.

3 Capolupo, L. *et al.* Sphingolipids control dermal fibroblast heterogeneity. *Science* **376**, eabh1623 (2022). https://doi.org:10.1126/science.abh1623.

4 van Meer, G. & van Genderen, I. L. Intracellular lipid distribution, transport, and sorting. A cell biologist's need for physicochemical information. *Subcell Biochem* **23**, 1-24 (1994).

5 Hanada, K. *et al.* Molecular machinery for non-vesicular trafficking of ceramide. *Nature* **426**, 803-809 (2003). https://doi.org:10.1038/nature02188.
6 Maeda, K. *et al.* Interactome map uncovers phosphatidylserine transport by oxysterol-binding proteins. *Nature* **501**, 257-261 (2013). https://doi.org:nature12430 [pii] 10.1038/nature12430.
7 Stefan, C. J. *et al.* Osh proteins regulate phosphoinositide metabolism at ER-plasma membrane contact sites. *Cell* **144**, 389-401 (2011). https://doi.org:10.1016/j.cell.2010.12.034
8 Mesmin, B. *et al.* A four-step cycle driven by PI(4)P hydrolysis directs sterol/PI(4)P exchange by the ER-Golgi tether OSBP. *Cell* **155**, 830-843 (2013). https://doi.org:10.1016/j.cell.2013.09.056.
9 Kono, N. *et al.* Impaired alpha-TTP-PIPs interaction underlies familial vitamin E deficiency. *Science* **340**, 1106-1110 (2013). https://doi.org:10.1126/science.1233508.
10 Chiapparino, A., Maeda, K., Turei, D., Saez-Rodriguez, J. & Gavin, A. C. The orchestra of lipid-transfer proteins at the crossroads between metabolism and signaling. *Prog Lipid Res* **61**, 30-39 (2016). https://doi.org:10.1016/j.plipres.2015.10.004.
11 Wong, L. H., Gatta, A. T. & Levine, T. P. Lipid transfer proteins: the lipid commute via shuttles, bridges and tubes. *Nat Rev Mol Cell Biol* **20**, 85-101 (2019). https://doi.org:10.1038/s41580-018-0071-5.
12 Peretti, D., Kim, S., Tufi, R. & Lev, S. Lipid Transfer Proteins and Membrane Contact Sites in Human Cancer. *Front Cell Dev Biol* **7**, 371 (2019). https://doi.org:10.3389/fcell.2019.00371
13 Moser von Filseck, J. *et al.* INTRACELLULAR TRANSPORT. Phosphatidylserine transport by ORP/Osh proteins is driven by phosphatidylinositol 4-phosphate. *Science* **349**, 432-436 (2015). https://doi.org:10.1126/science.aab1346.
14 Furst, W. & Sandhoff, K. Activator proteins and topology of lysosomal sphingolipid catabolism. *Biochim Biophys Acta* **1126**, 1-16 (1992).
15 Wang, P. Y., Liu, P., Weng, J., Sontag, E. & Anderson, R. G. A cholesterol-regulated PP2A/HePTP complex with dual specificity ERK1/2 phosphatase activity. *EMBO J* **22**, 2658-2667 (2003). https://doi.org:10.1093/emboj/cdg255.
16 Wong, L. H., Copic, A. & Levine, T. P. Advances on the Transfer of Lipids by Lipid Transfer Proteins. *Trends Biochem Sci* **42**, 516-530 (2017). https://doi.org:10.1016/j.tibs.2017.05.001
17 Koriyama, H., Nakagami, H., Katsuya, T. & Morishita, R. (ed Roya Kelishadi) (InTech, 2012).
18 Sahlberg, K. K. *et al.* The HER2 amplicon includes several genes required for the growth and survival of HER2 positive breast cancer cells. *Mol Oncol* **7**, 392-401 (2013). https://doi.org:10.1016/j.molonc.2012.10.012.
19 Guijas, C. *et al.* METLIN: A Technology Platform for Identifying Knowns and Unknowns. *Anal Chem* **90**, 3156-3164 (2018). https://doi.org:10.1021/acs.analchem.7b04424.
20 Aimo, L. *et al.* The SwissLipids knowledgebase for lipid biology. *Bioinformatics* **31**, 2860-2866 (2015). https://doi.org:10.1093/bioinformatics/btv285.
21 Fahy, E. *et al.* Update of the LIPID MAPS comprehensive classification system for lipids. *J Lipid Res* **50 Suppl**, S9-14 (2009). https://doi.org:10.1194/jlr.R800095-JLR200.
22 Ovcacikova, M., Lisa, M., Cifkova, E. & Holcapek, M. Retention behavior of lipids in reversed-phase ultrahigh-performance liquid chromatography-electrospray ionization mass spectrometry. *J Chromatogr A* **1450**, 76-85 (2016). https://doi.org:10.1016/j.chroma.2016.04.082.
23 Kofeler, H. C. *et al.* Quality control requirements for the correct annotation of lipidomics data. *Nat Commun* **12**, 4771 (2021). https://doi.org:10.1038/s41467-021-24984-y.
24 Danne-Rasche, N., Coman, C. & Ahrends, R. Nano-LC/NSI MS Refines Lipidomics by Enhancing Lipid Coverage, Measurement Sensitivity, and Linear Dynamic Range. *Anal Chem* **90**, 8093-8101 (2018). https://doi.org:10.1021/acs.analchem.8b01275.
25 Aicheler, F. *et al.* Retention Time Prediction Improves Identification in Nontargeted Lipidomics Approaches. *Anal Chem* **87**, 7698-7704 (2015). https://doi.org:10.1021/acs.analchem.5b01139.

26 Appala, K., Bimpeh, K., Freeman, C. & Hines, K. M. Recent applications of mass spectrometry in bacterial lipidomics. *Anal Bioanal Chem* **412**, 5935-5943 (2020). https://doi.org:10.1007/s00216-020-02541-8.
27 Vanni, S., Riccardi, L., Palermo, G. & De Vivo, M. Structure and Dynamics of the Acyl Chains in the Membrane Trafficking and Enzymatic Processing of Lipids. *Acc Chem Res* **52**, 3087-3096 (2019). https://doi.org:10.1021/acs.accounts.9b00134.
28 Steinhoff, J. S., Lass, A. & Schupp, M. Biological Functions of RBP4 and Its Relevance for Human Diseases. *Front Physiol* **12**, 659977 (2021). https://doi.org:10.3389/fphys.2021.659977.
29 Ile, K. E., Schaaf, G. & Bankaitis, V. A. Phosphatidylinositol transfer proteins and cellular nanoreactors for lipid signaling. *Nat Chem Biol* **2**, 576-583 (2006). https://doi.org:10.1038/nchembio835.
30 Ebner, M. *et al.* Nutrient-regulated control of lysosome function by signaling lipid conversion. *Cell* **186**, 5328-5346 e5326 (2023). https://doi.org:10.1016/j.cell.2023.09.027.
31 Ile, K. E. *et al.* Zebrafish class 1 phosphatidylinositol transfer proteins: PITPbeta and double cone cell outer segment integrity in retina. *Traffic* **11**, 1151-1167 (2010). https://doi.org:10.1111/j.1600-0854.2010.01085.x.
32 Gong, B. *et al.* A Golgi-derived vesicle potentiates PtdIns4P to PtdIns3P conversion for endosome fission. *Nat Cell Biol* **23**, 782-795 (2021). https://doi.org:10.1038/s41556-021-00704-y.
33 Pemberton, J. G., Kim, Y. J. & Balla, T. Integrated regulation of the phosphatidylinositol cycle and phosphoinositide-driven lipid transport at ER-PM contact sites. *Traffic* **21**, 200-219 (2020). https://doi.org:10.1111/tra.12709.
34 Kim, Y. J. *et al.* Metabolic routing maintains the unique fatty acid composition of phosphoinositides. *Embo Rep* **23**, e54532 (2022). https://doi.org:10.15252/embr.202154532
35 Hullin-Matsuda, F. *et al.* De novo biosynthesis of the late endosome lipid, bis(monoacylglycero)phosphate. *J Lipid Res* **48**, 1997-2008 (2007). https://doi.org:10.1194/jlr.M700154-JLR200
36 Brocard, C. & Hartig, A. Peroxisome targeting signal 1: is it really a simple tripeptide? *Biochim Biophys Acta* **1763**, 1565-1573 (2006). https://doi.org:10.1016/j.bbamcr.2006.08.022
37 Skogsberg, J. *et al.* Transcriptional profiling uncovers a network of cholesterol-responsive atherosclerosis target genes. *PLoS Genet* **4**, e1000036 (2008). https://doi.org:10.1371/journal.pgen.1000036
38 Wang, W. *et al.* Proteomic analysis of murine testes lipid droplets. *Sci Rep* **5**, 12070 (2015). https://doi.org:10.1038/srep12070
39 Chung, J. *et al.* INTRACELLULAR TRANSPORT. PI4P/phosphatidylserine countertransport at ORP5- and ORP8-mediated ER-plasma membrane contacts. *Science* **349**, 428-432 (2015). https://doi.org:10.1126/science.aab1370
40 Ghai, R. *et al.* ORP5 and ORP8 bind phosphatidylinositol-4, 5-biphosphate (PtdIns(4,5)P (2)) and regulate its level at the plasma membrane. *Nat Commun* **8**, 757 (2017). https://doi.org:10.1038/s41467-017-00861-5
41 Mochizuki, S., Miki, H., Zhou, R. & Noda, Y. The involvement of oxysterol-binding protein related protein (ORP) 6 in the counter-transport of phosphatidylinositol-4-phosphate (PI4P) and phosphatidylserine (PS) in neurons. *Biochem Biophys Rep* **30**, 101257 (2022). https://doi.org:10.1016/j.bbrep.2022.101257
42 Bankaitis, V. A., Mousley, C. J. & Schaaf, G. The Sec14 superfamily and mechanisms for crosstalk between lipid metabolism and lipid signaling. *Trends Biochem Sci* **35**, 150-160 (2010). https://doi.org:10.1016/j.tibs.2009.10.008
43 Zingg, J. M., Libinaki, R., Meydani, M. & Azzi, A. Modulation of phosphorylation of tocopherol and phosphatidylinositol by hTAP1/SEC14L2-mediated lipid exchange. *PLoS One* **9**, e101550 (2014). https://doi.org:10.1371/journal.pone.0101550

44 Tripathi, A., Nile, A. H. & Bankaitis, V. A. Sec14-like phosphatidylinositol-transfer proteins and diversification of phosphoinositide signalling outcomes. *Biochem Soc Trans* **42**, 1383-1388 (2014). https://doi.org:10.1042/BST20140187
45 Theodore Alexandrov, K. O., Andrew Palmer, Vitaly Kovalev, Artem Tarasov, Lachlan Stuart, Renat Nigmetzianov, Dominik Fay, Key METASPACE contributors, Mathieu Gaudin, Cristina Gonzalez Lopez, Marina Vetter, John Swales, Mark Bokhart, Mario Kompauer, James McKenzie, Luca Rappez, Dusan Velickovic, Regis Lavigne, Guanshi Zhang, Dinaiz Thinagaran, Elisa Ruhland, Marta Sans, Sergio Triana, Denis Abu Sammour, Sarah Aboulmagd, Charlotte Bagger, Nicole Strittmatter, Angelos Rigopoulos, Erin Gemperline, Asta Maria Joensen, Benedikt Geier, Christine Quiason, Eric Weaver, Mridula Prasad, Benjamin Balluff, Konstantin Nagornov, Lingjun Li, Michael Linscheid, Carsten Hopf, Dimitri Heintz, Manuel Liebeke, Bernhard Spengler, Berin Boughton, Christian Janfelt, Kumar Sharma, Charles Pineau, Christopher Anderton, Shane Ellis, Michael Becker, József Pánczél, Georges Da Violante, David Muddiman, Richard Goodwin, Livia Eberlin, Zoltan Takats, Sheerin Shahidi-Latham. METASPACE: A community-populated knowledge base of spatial metabolomes in health and disease. *bioRxiv preprint* (2019). https://doi.org:https://doi.org/10.1101/539478
46 Manders, E. M. M., Verbeek, F. J. & Aten, J. A. Measurement of co-localization of objects in dual-colour confocal images. *J Microsc* **169**, 375-382 (1993). https://doi.org:10.1111/j.1365-2818.1993.tb03313.x
47 Yamaji, T. & Hanada, K. Sphingolipid metabolism and interorganellar transport: localization of sphingolipid enzymes and lipid transfer proteins. *Traffic* **16**, 101-122 (2015). https://doi.org:10.1111/tra.12239
48 Hussain, M. M., Rava, P., Walsh, M., Rana, M. & Iqbal, J. Multiple functions of microsomal triglyceride transfer protein. *Nutr Metab (Lond)* **9**, 14 (2012). https://doi.org:10.1186/1743-7075-9-14
49 Kumagai, K. & Hanada, K. Structure, functions and regulation of CERT, a lipid-transfer protein for the delivery of ceramide at the ER-Golgi membrane contact sites. *FEBS Lett* **593**, 2366-2377 (2019). https://doi.org:10.1002/1873-3468.13511
50 Kumagai, K. *et al.* CERT mediates intermembrane transfer of various molecular species of ceramides. *J Biol Chem* **280**, 6488-6495 (2005). https://doi.org:10.1074/jbc.M409290200
51 Hannun, Y. A. & Obeid, L. M. Many ceramides. *J Biol Chem* **286**, 27855-27862 (2011). https://doi.org:10.1074/jbc.R111.254359
52 Hussain, M. M., Jin, W. & Jiang, X. C. Mechanisms involved in cellular ceramide homeostasis. *Nutr Metab (Lond)* **9**, 71 (2012). https://doi.org:10.1186/1743-7075-9-71
53 Halter, D. *et al.* Pre- and post-Golgi translocation of glucosylceramide in glycosphingolipid synthesis. *J Cell Biol* **179**, 101-115 (2007). https://doi.org:10.1083/jcb.200704091
54 Simanshu, D. K. *et al.* Non-vesicular trafficking by a ceramide-1-phosphate transfer protein regulates eicosanoids. *Nature* **500**, 463-467 (2013). https://doi.org:10.1038/nature12332
55 D'Angelo, G. *et al.* Vesicular and non-vesicular transport feed distinct glycosylation pathways in the Golgi. *Nature* **501**, 116-120 (2013). https://doi.org:10.1038/nature12423
56 Malinina, L., Malakhova, M. L., Teplov, A., Brown, R. E. & Patel, D. J. Structural basis for glycosphingolipid transfer specificity. *Nature* **430**, 1048-1053 (2004). https://doi.org:10.1038/nature02856
57 Rao, C. S., Lin, X., Pike, H. M., Molotkovsky, J. G. & Brown, R. E. Glycolipid transfer protein mediated transfer of glycosphingolipids between membranes: a model for action based on kinetic and thermodynamic analyses. *Biochemistry* **43**, 13805-13815 (2004). https://doi.org:10.1021/bi0492197
58 Dean, A. W. & Glasgow, B. J. Mass spectrometric identification of phospholipids in human tears and tear lipocalin. *Invest Ophthalmol Vis Sci* **53**, 1773-1782 (2012). https://doi.org:10.1167/iovs.11-9419
59 Omae, F. *et al.* DES2 protein is responsible for phytoceramide biosynthesis in the mouse small intestine. *Biochem J* **379**, 687-695 (2004). https://doi.org:10.1042/BJ20031425

60 Lachkar, F., Ferre, P., Foufelle, F. & Papaioannou, A. Dihydroceramides: their emerging physiological roles and functions in cancer and metabolic diseases. *Am J Physiol Endocrinol Metab* **320**, E122-E130 (2021). https://doi.org:10.1152/ajpendo.00330.2020

61 Enomoto, A. *et al.* Dihydroceramide:sphinganine C-4-hydroxylation requires Des2 hydroxylase and the membrane form of cytochrome b5. *Biochem J* **397**, 289-295 (2006). https://doi.org:10.1042/BJ20051938

62 Megha, Sawatzki, P., Kolter, T., Bittman, R. & London, E. Effect of ceramide N-acyl chain and polar headgroup structure on the properties of ordered lipid domains (lipid rafts). *Biochim Biophys Acta* **1768**, 2205-2212 (2007). https://doi.org:10.1016/j.bbamem.2007.05.007

63 Levy, M. & Futerman, A. H. Mammalian ceramide synthases. *IUBMB Life* **62**, 347-356 (2010). https://doi.org:10.1002/iub.319

64 Watson, P. & Stephens, D. J. ER-to-Golgi transport: form and formation of vesicular and tubular carriers. *Biochim Biophys Acta* **1744**, 304-315 (2005). https://doi.org:10.1016/j.bbamcr.2005.03.003

65 Mahmoud Moqadam, P. G., Reza Talandashti, Antonella Chiapparino, Kevin Titeca, Anne-Claude Gavin, Nathalie Reuter. A Mechanistic Model for the Release of Ceramide from the CERT START Domain. *bioRxiv preprint* (2023). https://doi.org:10.1101/2023.12.16.571968

66 Silverman, B. W. in *Density Estimation for Statistics and Data Analysis* 45 (Taylor and Francis Chapman and Hall/CRC, 1986).

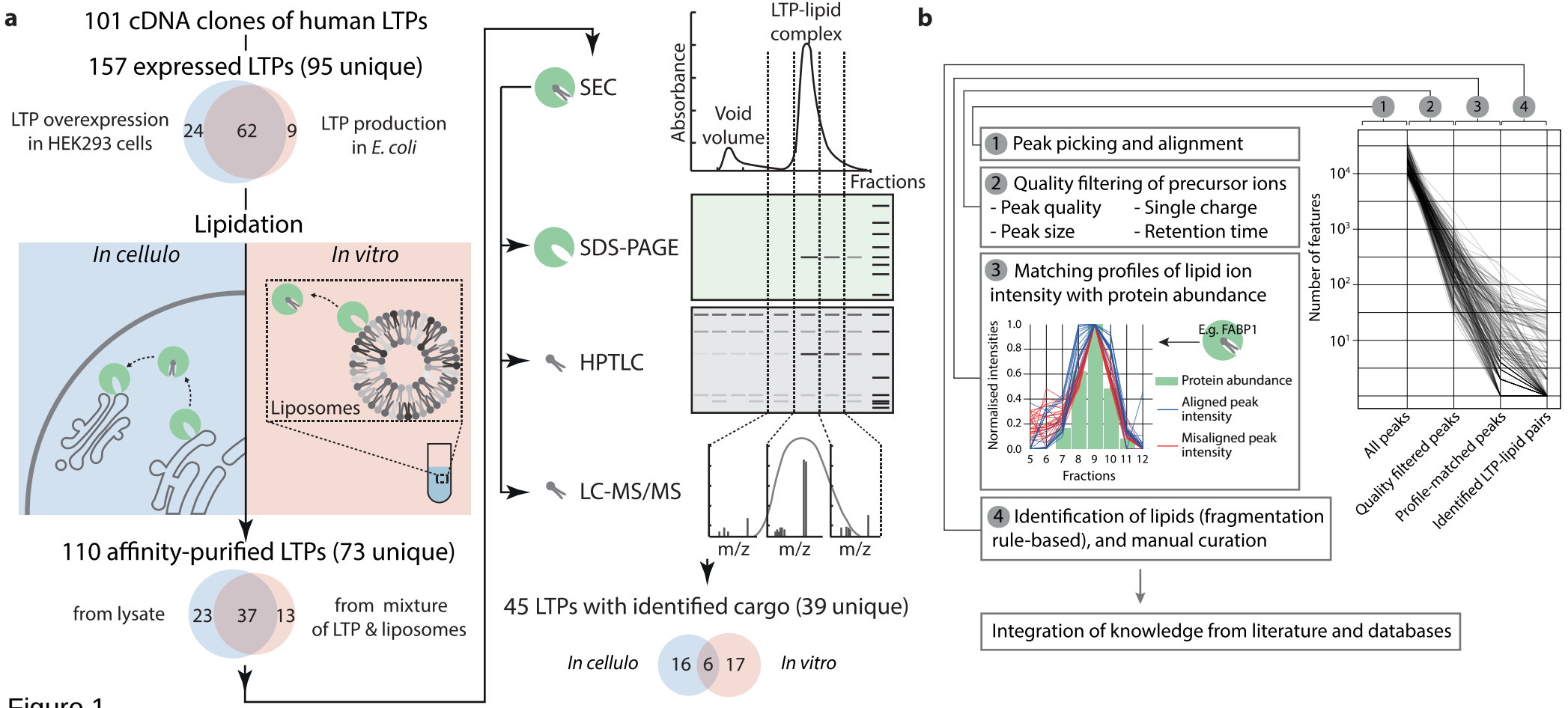
a
101 cDNA clones of human LTPs
157 expressed LTPs (95 unique)
LTP overexpression in HEK293 cells
24
62
9
LTP production in E. coli
Lipidation
In cellulo
In vitro
Liposomes
110 affinity-purified LTPs (73 unique)
from lysate
23
37
13
from mixture of LTP & liposomes
SEC
SDS-PAGE
HPTLC
LC-MS/MS
LTP-lipid complex
Absorbance
Void volume
Fractions
m/z
m/z
m/z
45 LTPs with identified cargo (39 unique)
In cellulo
16
6
17
In vitro
b
1 Peak picking and alignment
2 Quality filtering of precursor ions
- Peak quality
- Single charge
- Peak size
- Retention time
3 Matching profiles of lipid ion intensity with protein abundance
Normalised intensities
Fractions
E.g. FABP1
Protein abundance
Aligned peak intensity
Misaligned peak intensity
4 Identification of lipids (fragmentation rule-based), and manual curation
Number of features
All peaks
Quality filtered peaks
Profile-matched peaks
Identified LTP-lipid pairs
Integration of knowledge from literature and databases

Figure 1

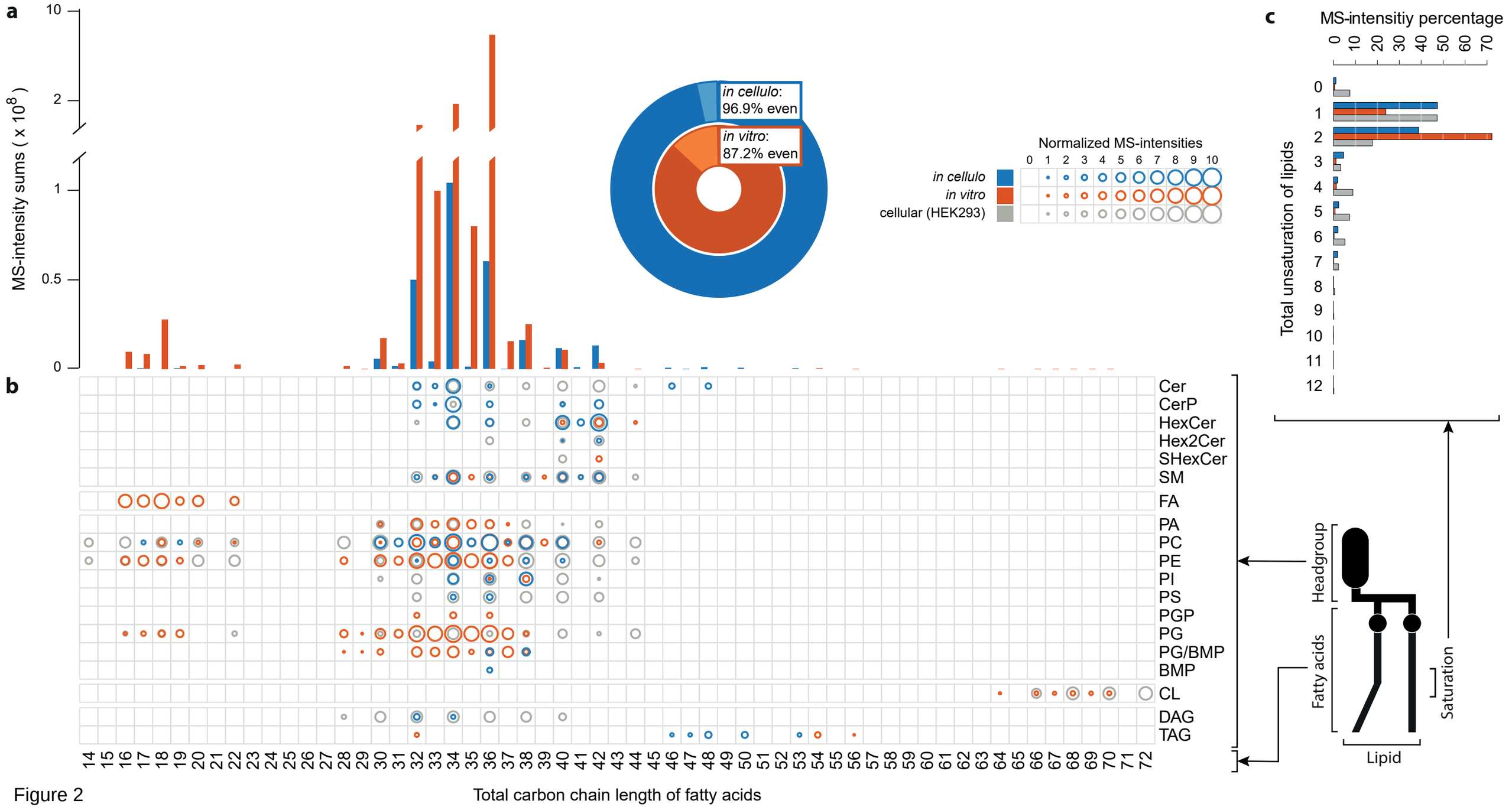
a
MS-intensity sums (x 10^8)
10
2
1
0.5
0
in cellulo:
96.9% even
in vitro:
87.2% even
Normalized MS-intensities
0 1 2 3 4 5 6 7 8 9 10
in cellulo
in vitro
cellular (HEK293)
c
MS-intensitiy percentage
0 10 20 30 40 50 60 70
Total unsaturation of lipids
0 1 2 3 4 5 6 7 8 9 10 11 12
b
Cer
CerP
HexCer
Hex2Cer
SHexCer
SM
FA
PA
PC
PE
PI
PS
PGP
PG
PG/BMP
BMP
CL
DAG
TAG
14 15 16 17 18 19 20 21 22 23 24 25 26 27 28 29 30 31 32 33 34 35 36 37 38 39 40 41 42 43 44 45 46 47 48 49 50 51 52 53 54 55 56 57 58 59 60 61 62 63 64 65 66 67 68 69 70 71 72
Total carbon chain length of fatty acids
Headgroup
Fatty acids
Saturation
Lipid

Figure 2

Figure 3

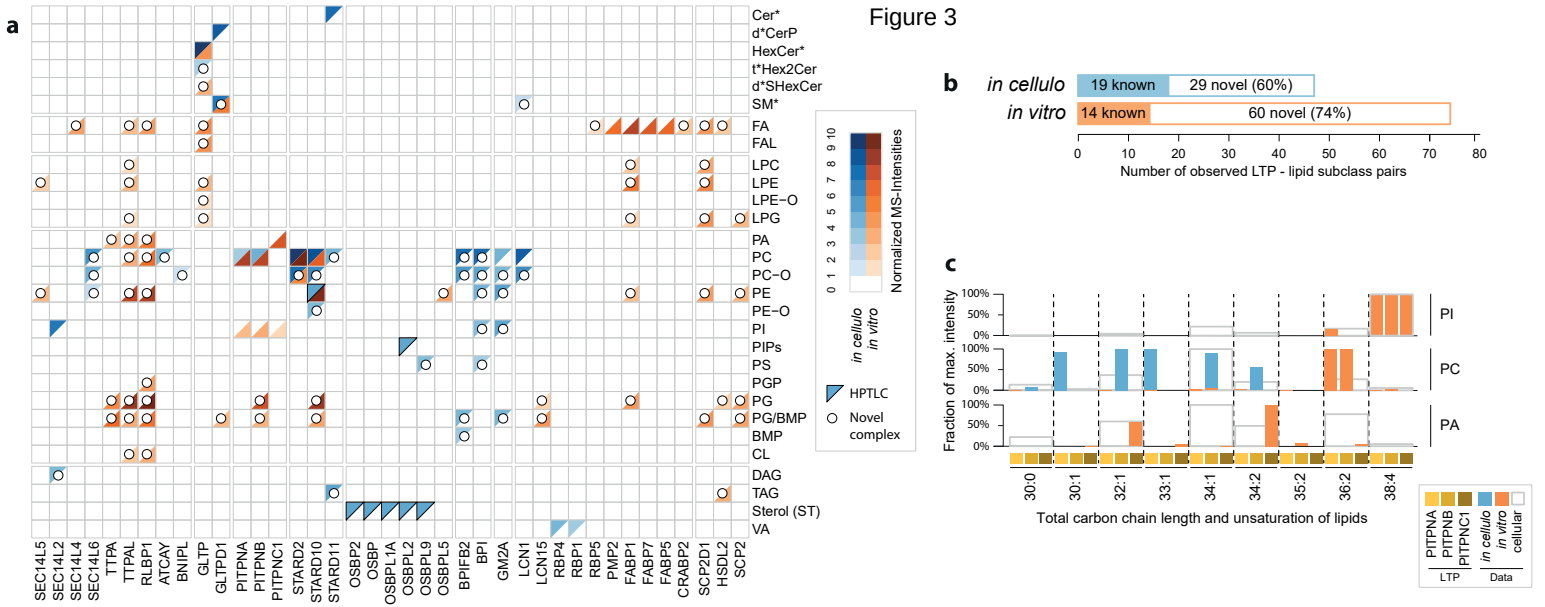
a
Cer*
d*CerP
HexCer*
t*Hex2Cer
d*SHexCer
SM*
FA
FAL
LPC
LPE
LPE−O
LPG
PA
PC
PC−O
PE
PE−O
PI
PIPs
PS
PGP
PG
PG/BMP
BMP
CL
DAG
TAG
Sterol (ST)
VA
SEC14L5
SEC14L2
SEC14L4
SEC14L6
TTPA
TTPAL
RLBP1
ATCAY
BNIPL
GLTP
GLTPD1
PITPNA
PITPNB
PITPNC1
STARD2
STARD10
STARD11
OSBP2
OSBP
OSBPL1A
OSBPL2
OSBPL9
OSBPL5
BPIFB2
BPI
GM2A
LCN1
LCN15
RBP4
RBP1
RBP5
PMP2
FABP1
FABP7
FABP5
CRABP2
SCP2D1
HSDL2
SCP2
CRAL-TRIO
GLTP
PITP
START
OSBP
BPI
ML
Lipocalin
SCP2
0 1 2 3 4 5 6 7 8 9 10
Normalized MS-Intensities
in cellulo
in vitro
HPTLC
Novel complex
b
in cellulo
19 known
29 novel (60%)
in vitro
14 known
60 novel (74%)
0 10 20 30 40 50 60 70 80
Number of observed LTP - lipid subclass pairs
c
Fraction of max. intensity
100%
50%
0%
PI
PC
PA
30:0
30:1
32:1
33:1
34:1
34:2
35:2
36:2
38:4
Total carbon chain length and unsaturation of lipids
PITPNA
PITPNB
PITPNC1
LTP
in cellulo
in vitro
cellular
Data

Figure 4

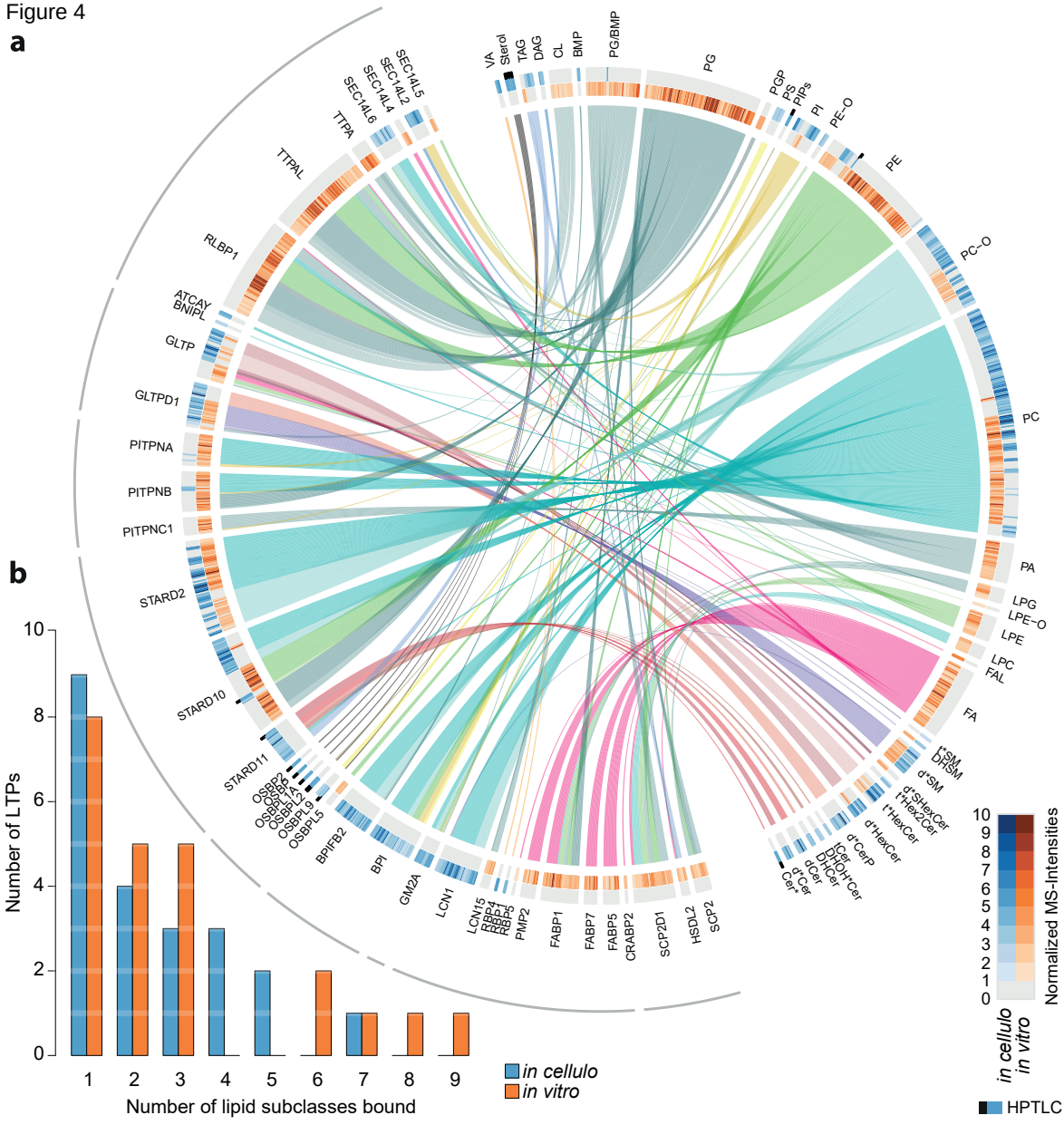
a
VA
Sterol
TAG
DAG
CL
BMP
PG/BMP
PG
PGP
PS
PIPs
PI
PE-O
PE
PC-O
PC
PA
LPG
LPE-O
LPE
LPC
FAL
FA
t-SM
DHSM
d-SM
d-SHexCer
t-HexCer
t-HexCer
d-HexCer
d-CerP
tCer
DHOHCer
DHCer
dCer
d-Cer
Cer+
SCP2
HSDL2
SCP2D1
CRABP2
FABP5
FABP7
FABP1
PMP2
RBP5
RBP1
RBP4
LCN15
LCN1
GM2A
BPI
BPIFB2
OSBPL5
OSBPL9
OSBPL2
OSBPL1A
OSBP2
OSBP
STARD11
STARD10
STARD2
PITPNC1
PITPNB
PITPNA
GLTPD1
GLTP
BNIPL
ATCAY
RLBP1
TTPAL
TTPA
SEC14L6
SEC14L4
SEC14L2
SEC14L5
b
Number of LTPs
Number of lipid subclasses bound
in cellulo
in vitro
Normalized MS-Intensities
HPTLC

Figure 5

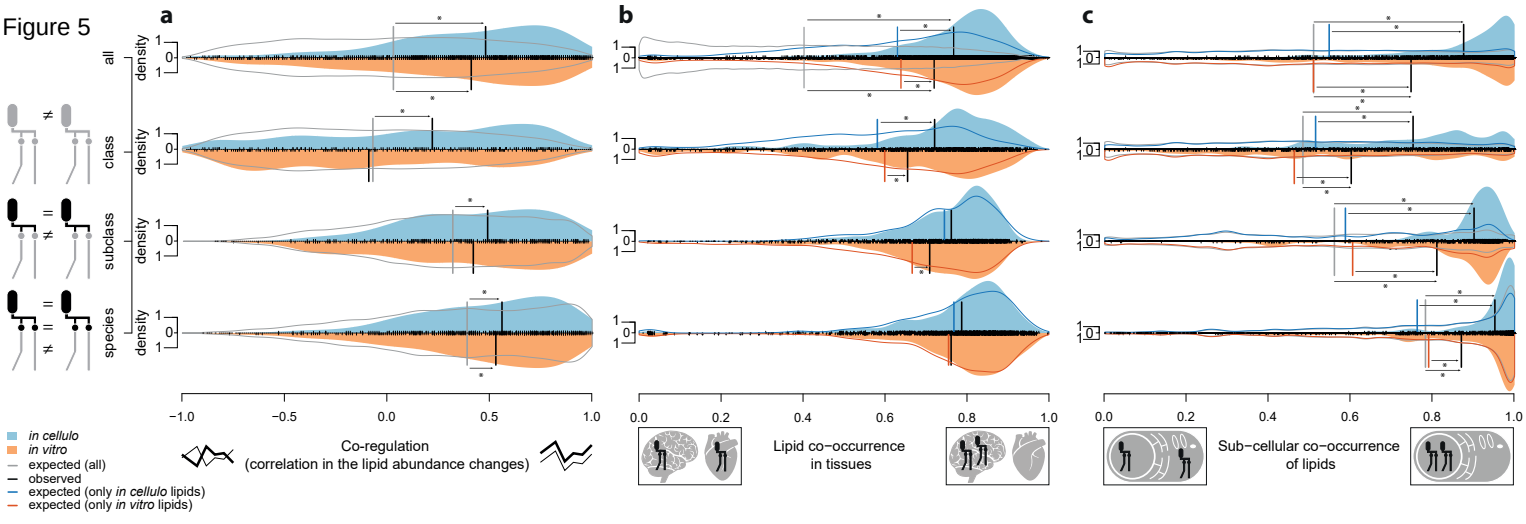
a
b
c
all
class
subclass
species
density
−1.0
−0.5
0.0
0.5
1.0
0.0
0.2
0.4
0.6
0.8
1.0
Co-regulation
(correlation in the lipid abundance changes)
Lipid co−occurrence
in tissues
Sub−cellular co−occurrence
of lipids
in cellulo
in vitro
expected (all)
observed
expected (only in cellulo lipids)
expected (only in vitro lipids)

Figure 6

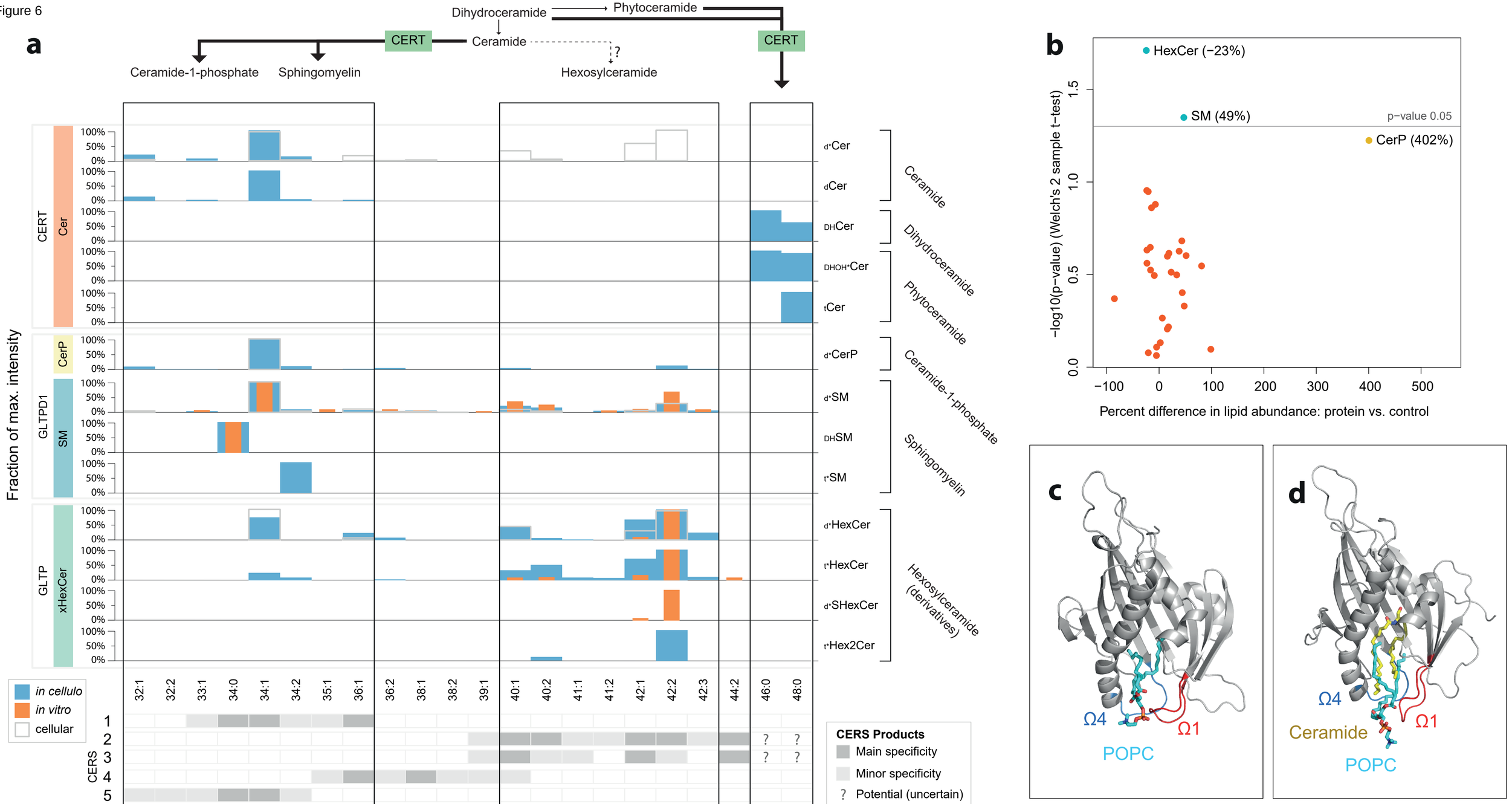
a
Dihydroceramide
Phytoceramide
CERT
Ceramide
CERT
Ceramide-1-phosphate
Sphingomyelin
?
Hexosylceramide
Fraction of max. intensity
CERT
Cer
CerP
GLTPD1
SM
GLTP
xHexCer
100%
50%
0%
d*Cer
dCer
DHCer
DHOH*Cer
tCer
d*CerP
d*SM
DHSM
t*SM
d*HexCer
t*HexCer
d*SHexCer
t*Hex2Cer
Ceramide
Dihydroceramide
Phytoceramide
Ceramide-1-phosphate
Sphingomyelin
Hexosylceramide (derivatives)
32:1
32:2
33:1
34:0
34:1
34:2
35:1
36:1
36:2
38:1
38:2
39:1
40:1
40:2
41:1
41:2
42:1
42:2
42:3
44:2
46:0
48:0
in cellulo
in vitro
cellular
CERS
1
2
3
4
5
6
?
CERS Products
Main specificity
Minor specificity
? Potential (uncertain)
b
HexCer (−23%)
SM (49%)
CerP (402%)
p−value 0.05
−log10(p−value) (Welch's 2 sample t−test)
0.0
0.5
1.0
1.5
−100
0
100
200
300
400
500
Percent difference in lipid abundance: protein vs. control
c
Ω4
Ω1
POPC
d
Ω4
Ω1
Ceramide
POPC